nature ecology & evolution

Article

https://doi.org/10.1038/s41559-022-01929-2

Arched footprints preserve the motions of fossil hominin feet

Received: 30 August 2022

Accepted: 7 October 2022

Published online: 05 January 2023

Check for updates

Kevin G. Hatala [1] ✉, Stephen M. Gatesy [2] & Peter L. Falkingham [3]

The longitudinal arch of the human foot is viewed as a pivotal adaptation for bipedal walking and running. Fossil footprints from Laetoli, Tanzania, and Ileret, Kenya, are believed to provide direct evidence of longitudinally arched feet in hominins from the Pliocene and Pleistocene, respectively. We studied the dynamics of track formation using biplanar X-ray, three-dimensional animation and discrete element particle simulation. Here, we demonstrate that longitudinally arched footprints are false indicators of foot anatomy; instead they are generated through a specific pattern of foot kinematics that is characteristic of human walking. Analyses of fossil hominin tracks from Laetoli show only partial evidence of this walking style, with a similar heel strike but a different pattern of propulsion. The earliest known evidence for fully modern human-like bipedal kinematics comes from the early Pleistocene Ileret tracks, which were presumably made by members of the genus *Homo*. This result signals important differences in the foot kinematics recorded at Laetoli and Ileret and underscores an emerging picture of locomotor diversity within the hominin clade.

Human bipedal locomotion is unique among living primates and has long been considered a primary trait that defines the hominin clade[1]. The longitudinal arch is often cited as an important evolutionary innovation of the human foot that contributed to proficient bipedal walking and adept endurance running in our fossil relatives[2–4]; there exists tremendous interest in the evolution of this distinctly human foot anatomy. However, skeletal fossils are typically fragmentary and soft tissues rarely preserve, making it difficult to interpret arch anatomy from hominin fossils. Fossil footprints provide an alternative, possibly more direct view of intact feet of living individuals. The 1978 discovery of hominin tracks (footprints) from 3.66 million years ago (Ma) at Laetoli, Tanzania, appeared to provide the oldest fossil evidence of longitudinal arches[5]. This interpretation has been supported repeatedly in the four decades since then[6–10]. Likewise, 1.5 Ma hominin tracks from Ileret, Kenya, are viewed as direct evidence of a longitudinally arched foot in at least one Pleistocene taxon[11]. Given the challenges of interpreting arches from fossil feet[12,13], the Laetoli and Ileret tracks are considered the least equivocal evidence for a deep history of longitudinally arched foot morphologies in hominin evolution.

Inferring longitudinally arched feet from longitudinally arched tracks (Fig. 1a–d) appears straightforward but the extent to which the topography of the deformed substrate reflects foot arch morphology has never been demonstrated. Here, we test this anatomical fidelity hypothesis by using a 'track ontogeny' approach[14–16] to elucidate the development of longitudinally arched footprints. In biplanar X-ray experiments, we used 85 skin markers to reconstruct the dynamic foot shape of four subjects walking across substrates spanning from a solid to compliant wet mud. To directly compare three-dimensional (3D) arch morphologies of feet and their resulting tracks, we developed a scale-free method for measuring their relative arch volumes (RAV; Fig. 1e–g). We then input experimentally derived and hypothetical animated foot models to drive particle-based substrate simulations to assess spatiotemporal aspects of the sediment deformation that leads to longitudinally arched tracks. Finally, we applied our findings to reinterpret fossil hominin tracks through the unique perspective afforded by this lens.

[1]Department of Biology, Chatham University, Pittsburgh, PA, USA. [2]Department of Ecology, Evolution, and Organismal Biology, Brown University, Providence, RI, USA. [3]School of Biological and Environmental Sciences, Liverpool John Moores University, Liverpool, UK.
✉e-mail: kevin.g.hatala@gmail.com

https://doi.org/10.1038/s41559-022-01929-2

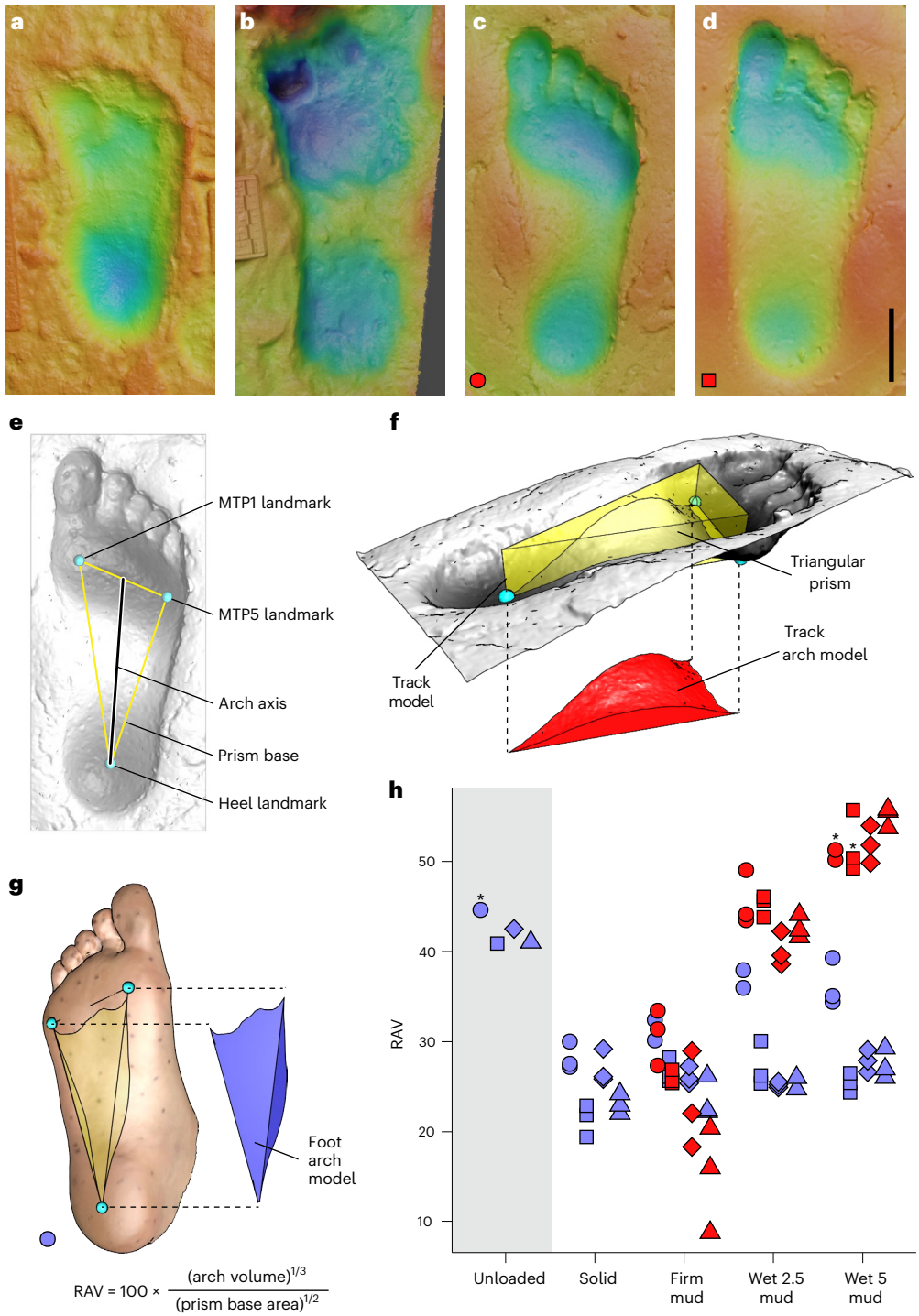

Fig. 1 | Arched hominin tracks in soft substrates do not faithfully record the feet that made them. a–**d**, Hominin tracks from Laetoli (**a**), Ileret (**b**) and our most-arched (**c**) and least-arched (**d**) experimental subjects all appear longitudinally arched. Colour scale spans 6 cm from dark blue to dark red. **e**, To quantify arch volumes, three landmarks (aqua spheres) define a triangular prism. **f**, The intersection between track model (grey) and prism (yellow) yields a track arch model (red). **g**, A comparable foot arch model (blue) can be derived from anatomical landmarks. Relative arch volumes (RAV) is calculated from the volume and prism base area of each arch model. **h**, Foot (blue) and track (red) RAV for four subjects' (four symbols) trials under five loading conditions (total $n = 85$). Compared to an unloaded state, midstance foot RAV was substantially reduced when walking across all four substrates. Track RAV varied with substrate deformability, from less than midstance foot RAV on 'firm' ground to almost doubling midstance foot RAV in the deepest wet mud. Asterisks indicate observations also shown in **c**, **d** and **g**.

Results and discussion

When we measured each experimental subject's foot at midstance, their anatomical foot RAVs were consistently much less than their unloaded resting foot RAVs across substrates. Track RAVs showed a directional trend, becoming more arched in substrates where subjects' feet sank deeper (Fig. 1h). Feet at midstance were notably less arched than all but their shallowest tracks, in which the foot did not sink deep enough for the plantar surface beneath the longitudinal arch to contact

completely the substrate. In deeper experimental tracks—which better resemble known fossil tracks from Laetoli and Ileret—track RAV was on average 1.85 times higher (range 1.3× to 2.1×) than foot RAV. Moreover, variation in foot RAV among our subjects confirmed that even the least-arched individual consistently produced considerably arched tracks in our softest, deepest, muds (Fig. 1h). In case this pattern that we observed among our four biplanar X-ray subjects was influenced by sample size, we also examined the correlation between track RAV and navicular height among a larger sample of footprints that were made by habitually barefoot people as part of a previously published experiment[17] (Supplementary Note 1 and Extended Data Fig. 1). There, we could statistically evaluate the correlation between track RAV and navicular height. We found that this relationship was not statistically significant, further demonstrating the disconnect between foot arch anatomy and track morphology.

The clear mismatch between the longitudinal arches of feet and tracks refutes the prevalent assumption that foot arch morphology can be directly reconstructed from fossil footprints[5–11]. Beyond demonstrating this inferential flaw, we discovered that track longitudinal arches originate and are shaped by the kinematics of the foot as it navigates a deforming substrate. By using particle simulations to visualize track ontogeny, we found that the track's longitudinal arch is shaped continuously throughout stance phase (Fig. 2a–d), with the proximal part forming soon after heel strike. Soft substrates allow the heel to rise as the forefoot continues to sink, leading track RAV to increase continuously throughout midstance. At 50% of stance phase, both the heel and forefoot are shallower than the maximum depths they reach earlier and later in stance, respectively, as substrate beneath the midfoot appears to support it. Following midstance, as the heel continues to rise and the forefoot pushes off, sediment travels backwards and upwards, enhancing the longitudinal arch left behind. Rather than duplicating static pedal anatomy, deep tracks more closely resemble the substrate volume swept by a cumulative sequence of foot poses (Fig. 2a,b, Extended Data Fig. 2 and Supplementary Note 2). Viewed through the lens of how they form, a deep and highly arched track thereby records an important biomechanical phenomenon.

When humans walk, the heel strikes the ground first, the forefoot pushes off at the end and a smooth transition occurs in between. This rotational motion pattern increases the effective length of the lower limb, thereby reducing costs of inverted pendulum bipedalism and increasing muscular efficacy for propulsive force generation[18,19] (Fig. 3a,b). We visualized this heel–sole–toe rollover in our experiments by calculating a sagittal pivot between those sole markers moving upwards and those moving downwards. On soft substrates, this pivot starts proximally and then translates distally from heel to toe, following a path akin to the centre of plantar pressure on solid ground (Fig. 3c). While we were unable to directly quantify forces or pressures in our experiments, others have demonstrated the kinetic correlates of the kinematic patterns that we observed[18]. As a consequence of these foot kinematics, regions of substrate descend and rise depending on the presence and motion of the interacting foot (Fig. 3d). For an exaggerated theoretical test, we also ran 3D particle simulations in which a rigid, rectangular model was animated with an anteriorly translating pivot following human-like motion (Fig. 3e). Even this flat-bottomed block created longitudinally ached tracks. A longitudinally arched fossil track therefore serves as evidence of similar bipedal foot kinematics in extinct hominins.

We measured longitudinal arch morphologies of Pliocene (Laetoli, Tanzania; 3.66 Ma), Pleistocene (Ileret, Kenya; 1.5 Ma) and Holocene (Walvis Bay, Namibia, ~400–500 yr BP) hominin tracks[5,11,20–23]. We compared these with our experimental human footprints made in deep mud (made by eight subjects, total $n = 53$) and with footprints produced in prior experiments by habitually unshod people[17] ($n = 36$ tracks from 17 subjects) and by chimpanzees walking bipedally[10] (made by two subjects; $n_1 = 22$, $n_2 = 21$). Chimpanzee tracks are less longitudinally arched than those of humans and their track RAVs are highly variable, irrespective of depth (Fig. 4a). This track RAV inconsistency probably reflects that chimpanzees use heel strikes but as part of their more variable bipedal foot kinematics[24,25]. Even when chimpanzee track RAVs approach values recorded in hominin tracks, their track arches differ substantially in shape and are easily distinguished (Extended Data Fig. 3 and Supplementary Note 3). By contrast, the Namibia and unshod human experimental track RAVs vary with footprint depth in a pattern congruous to that observed in our biplanar X-ray experiments. The Namibia tracks (made by two individuals; $n_1 = 13$ and $n_2 = 11$) were produced across variable substrate conditions[22], resulting in relative track depths that span roughly the same range as our experimental tracks. That Namibian and experimental human tracks follow similar trends offers confidence for mechanistic inferences in samples from other bipedal fossil hominins.

We analysed hominin tracks from three Laetoli trackways: G1 ($n = 11$), S1 ($n = 2$) and A ($n = 1$). Laetoli G1 and S1 tracks are longitudinally arched but their RAVs are notably smaller and more variable than similarly deep tracks measured from human experiments or from younger fossil sites (Fig. 4a). The S1 tracks are substantially larger[20] but their RAVs fall within the distribution of G1, suggesting that they record similar foot kinematics. The only Laetoli A track sufficiently cleared of matrix[23] (A3) is extremely flat, with a RAV far below our human data and much lower than all other fossil samples (Fig. 4a). Previous workers have proposed that the deep heel impressions of the G1 tracks may reflect evidence of a bipedal gait that included a human-like heel strike[19]. We can now confirm, on the basis of track ontogeny, that the longitudinally arched Laetoli G1 and S1 tracks preserve the earliest known evidence of a heel–sole–toe pattern of foot kinematics in the hominin fossil record.

However, a key distinction between Laetoli and modern human tracks is their pitch. All of the Laetoli G1 and S1 footprints have relatively deeper heel and shallower forefoot impressions (positive pitch), whereas at similar depths human tracks tend to have minimal pitch or be deepest in the forefoot (negative pitch)[8,22] (Fig. 4b). On the basis of track ontogeny, the Laetoli asymmetry could result from kinematic differences in heel strike or push-off. Of these, we believe a different manner of propulsion is both more plausible and more concordant with the skeletal morphology of *Australopithecus afarensis*, the presumed creator of the Laetoli G1 and S1 tracks[7,20]. Specifically, calcaneal robusticity of *A. afarensis* appears well-suited for repetitive stresses similar to those experienced during human bipedalism[26,27]. The *A. afarensis* lateral metatarsals and transverse arch configuration have been interpreted as potential evidence of different propulsive mechanics than are seen in modern humans[28,29]. Likewise, tarsal morphology may confer greater hallucial mobility, resulting in less stereotyped propulsive loading postures[30,31], which could explain the variation observed in Laetoli RAV measurements (Fig. 4a). While isolated analyses of skeletal fossils have generated conflicting interpretations about whether the *A. afarensis* foot functioned like that of a modern human[26–31], our analysis of the arched Laetoli footprints provides a unique kinematic synthesis. Brought into view through this new lens is a pattern of foot function and bipedal locomotion that was human-like in some ways yet still importantly different.

In contrast, 1.5 Ma tracks from Ileret, Kenya, preserve the earliest evidence for a fully human-like pattern of foot kinematics. Tracks from Ileret (total $n = 4$ from three trackways) have RAVs where we would expect similarly deep modern human tracks to fall (Fig. 4a). These data provide new evidence to support inferences of human-like foot kinematics in *Homo erectus*[11,17]. We emphasize, however, that our track ontogeny results simultaneously invalidate direct association between arched footprint morphology and arched foot anatomy at Ileret[11]. In contrast with the Laetoli examples above, it appears that the Ileret tracks are fully consistent with not only a heel–sole–toe rollover pattern but also a pattern of forefoot propulsion closer to that observed in modern humans. While Ileret tracks may be even more

https://doi.org/10.1038/s41559-022-01929-2

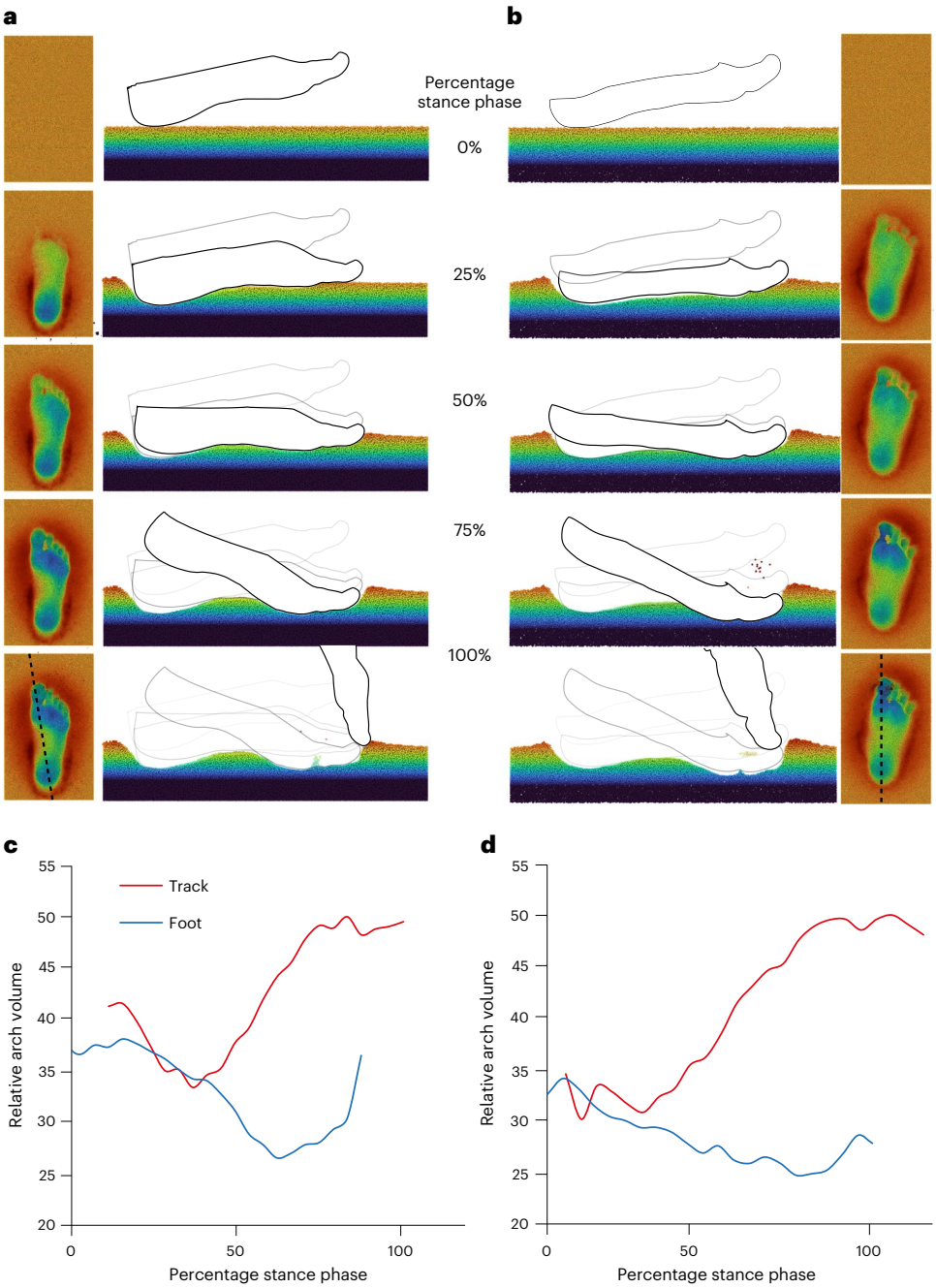

Fig. 2 | Discrete element method (DEM) simulations of arched track ontogeny. a,**b**, Simulations for a relatively high-arched (**a**) and low-arched (**b**) subject on 'wet 5' mud. Top views of simulated tracks and longitudinal sections through 3D animated foot models (black/grey outlines) and substrate (coloured particles) are shown at five instances during the stance phase of walking on 'wet 5' mud. Dashed lines show the longitudinal section planes. **c**,**d**, Dynamic RAVs for the feet (blue) and simulated tracks (red) diverge in mid-late stance in both the relatively high-arched (**c**) and low-arched (**d**) subjects. Despite different foot arch anatomies, both subjects form highly arched tracks.

negatively pitched than our experimental human sample (Fig. 4b), they are also slightly deeper. Prior studies of fossil and modern human tracks have indicated that tracks become more negatively pitched with depth[22].

The experimental evidence presented here demonstrates that the longitudinal arches of footprints develop as a consequence of heel–sole–toe foot kinematics, irrespective of foot anatomy. In modern humans, both longitudinally arched feet and flat feet are capable of achieving the minimum threshold of foot stiffness required for a foot to move in this way[32]. That threshold is perhaps achieved through the stiffness provided by the foot skeleton's transverse arch[29], although it may be impossible to generate modern human-like propulsive forces without other hard and/or soft tissue mechanisms for further stiffening the foot. For example, humans exhibit substantial control of longitudinal arch stiffness via intrinsic foot muscles[33–35]. On the basis of skeletal fossils, it remains an open question when and how these foot stiffening mechanisms evolved in hominins. The results of our track analyses suggest that important changes to foot anatomy and function occurred at or before the emergence of the genus *Homo*, where a suite of postcranial changes[36] could correspond to selective

https://doi.org/10.1038/s41559-022-01929-2

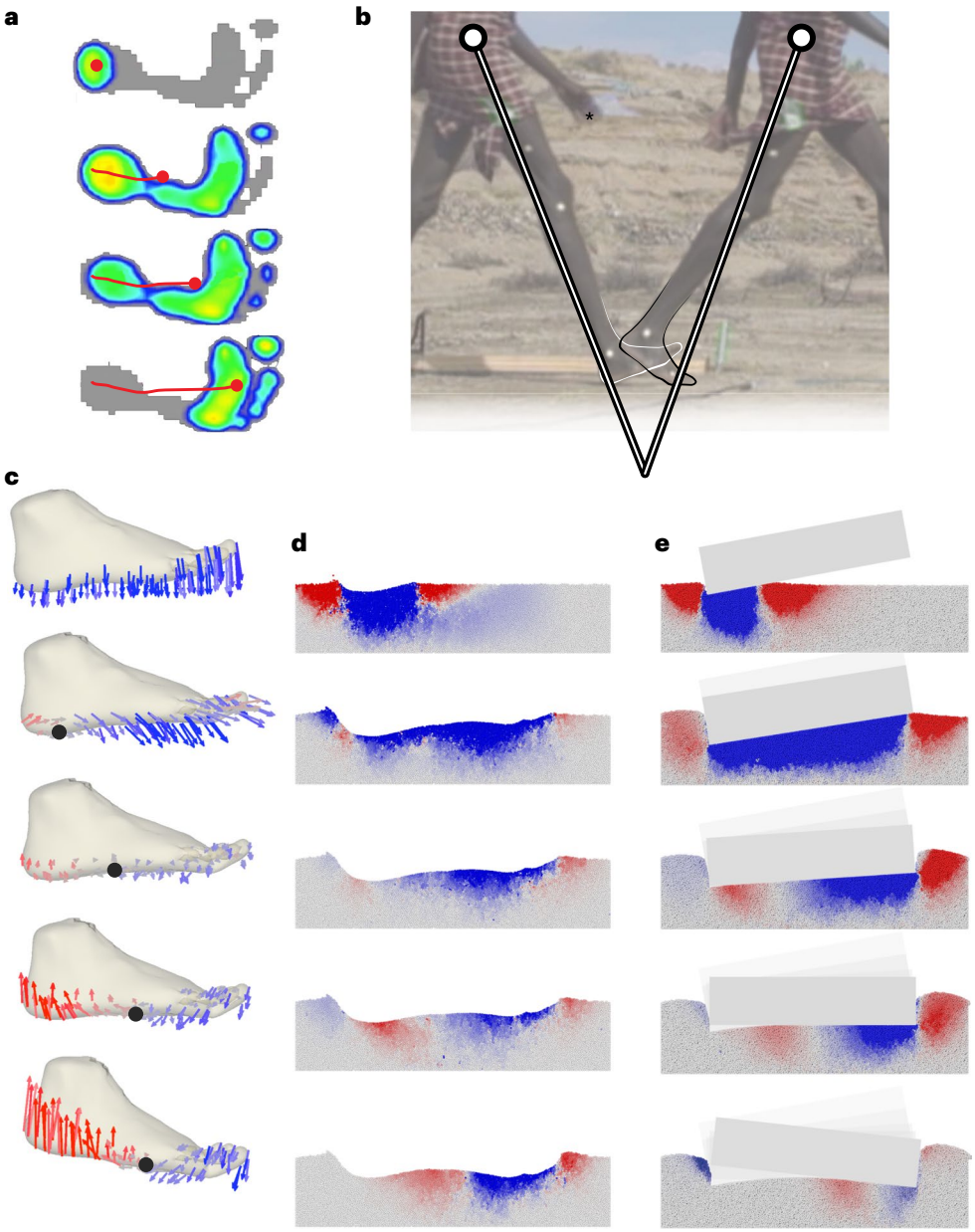

Fig. 3 | Arched tracks arise from human foot kinematics. a, Data from rigid instruments, such as pressure pads or force plates, document translation of the foot's centre of pressure from heel to toe during a step. **b**, Centre of pressure translation is thought to increase the effective length of the limb pendulum (photo credit, K.G.H.). **c**, Frame–frame displacements of 85 skin markers reveal a similar anterior translation of the pivot between the descending (blue vectors) and ascending (red vectors) portions of the foot through time. Vectors magnified ×20 in all but the first pose (×2). **d**, Similar displacement colouration of simulated mud documents synchrony between translation of the pivot of the sole and ontogeny of the arch of the track. **e**, Applying an advancing pivot kinematic pattern to a rigid flat-sided block (grey) in DEM-simulated mud produces a longitudinally arched track.

influences of locomotor behaviours such as long-distance walking or endurance running[4].

Ultimately, our results demonstrate that deciphering the mechanistic origins of fossil hominin footprints can clarify and contextualize analyses of skeletal morphology and elucidate the locomotor biomechanics of fossil hominins. In this case, the longitudinal arches of hominin tracks offer invaluable and otherwise inaccessible information on hominin locomotion, yet not in the manner that has long been assumed.

Methods

Research activities involving human subjects complied with all relevant ethical regulations and followed protocols approved by the Institutional Review Boards of Brown University and Chatham University.

Biplanar X-ray experimental setup

All biplanar X-ray experiments took place at the W.M. Keck Foundation XROMM Facility at Brown University and our methods for data collection have been described previously[16]. An elevated trackway measuring approximately 6 m long, 0.6 m wide and 0.5 m tall was constructed using wooden platforms at either end and a modified stone slab table in between. Three rigid panels of closed-cell extruded polystyrene (EPS) were placed upon the stone slab table (two panels 5 cm thick; one panel 2.5 cm thick). A diamond-shaped recess was cut into the centre of these foam panels, such that a $30 \times 30 \times 14.5\ cm^3$ foam container could be securely embedded at their centre. Biplanar X-ray equipment was focused at the centre of this trackway, such that X-ray beams intersected the diamond-shaped recess. Two telescoping ceiling cranes

https://doi.org/10.1038/s41559-022-01929-2

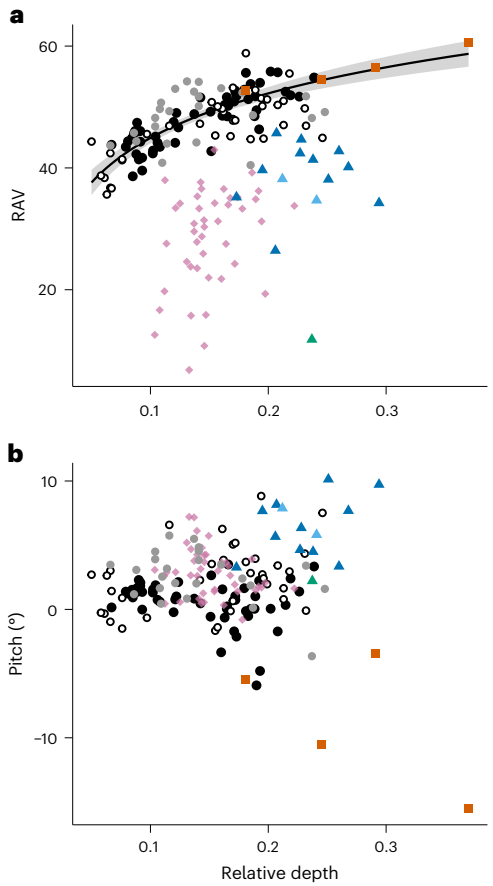

Fig. 4 | Fossil RAV and implications for heel–sole–toe kinematic pattern. **a**, Fossil human tracks from Namibia (grey circles) and tracks from prior human experiments (open circles) closely match the RAV–depth relationship observed in our experiments (black circles, original data; black line and grey outline, logarithmic fit of experimental track RAV versus relative depth, with 95% confidence interval around conditional mean; slope = 10.54, intercept = 69.21, *F*-statistic = 114.9, $P = 1.14 \times 10^{-14}$, adjusted $R^2 = 0.69$). Relative depth (*x* axis) is depth measured at the midpoint of the track arch model's longitudinal axis, divided by the length of that axis. RAVs of Ileret tracks (orange squares) fall within the range expected from similarly deep human tracks. Laetoli G1 (dark blue triangles) and S1 tracks (light blue triangles) have lower RAV than similarly deep human tracks, while Laetoli A (green triangles) is still lower than those. Chimpanzee tracks (pink diamonds) are highly variable but show lower RAV than do human tracks. **b**, As human tracks get deeper, they are typically either minimally pitched or negatively pitched. The Laetoli tracks diverge from this pattern and are positively pitched. One Ileret track is very negatively pitched, a pattern that has been observed in other fossil and modern human tracks in very deep mud[22]. Colour and symbol scheme same as **a**.

were attached to X-ray tubes that projected collimated X-rays that were received by two 40.64 cm diameter image intensifiers that were themselves attached to mobile bases. X-ray emitters were placed 134 cm from image intensifiers, at an angle of ~90° to each other and pitched upwards 10° relative to the ground plane. Video recordings were collected from the image intensifiers by two Phantom v.10 high-speed digital cameras (Vision Research), at a resolution of 1,760 × 1,760 pixels[2]. A third camera (Phantom v.9.1) recorded standard light video of each subject's right foot from a perspective perpendicular to the trackway (Extended Data Fig. 4). All three cameras were synchronized to within 4 µs and recorded at 50 frames per second (fps), with 2,000 µs exposure times. The Phantom cameras' Extreme Dynamic Range was set to between 300 and 500 µs, adjusting to improve visibility as needed for different substrate conditions. Pulsed X-rays (2 ms pulse widths) were transmitted at voltages of 60–90 kV and currents of 250–400 mA, with higher energies used for wetter/denser substrates. When using higher energies for wetter/denser substrates, compensating filters consisting of plasticine blocks were placed on the top halves of X-ray collimators to reduce exposure above the substrate surface.

Four configurations of the trackway were used to conduct experiments on four different substrates. In one setup, a rigid carbon fibre platform (70 × 30.5 × 2.7 cm^3) was placed on top of the diamond-shaped recess and 2.5 cm thick EPS panels (~2.4 × 1.2 m^2) were placed along the remainder of the trackway such that its surface was flush and level. In the remaining three, a square foam container (30 × 30 × 14.5 cm^3, with 3 cm walls) was placed within the diamond-shaped recess and filled with 11.5 cm of a deformable substrate[16]. Triangular foam wedges were placed within the medial and lateral corners of the three containers (to reduce the amount of substrate to improve the clarity of X-ray videos) reducing their widths to 22 cm (maximum length was ~34 cm). The deformable substrates that filled the containers included a 24:5:9 volumetric ratio of 60 µm glass bubbles (Type K15, 3M Co.), modelling clay and water, which was then mixed with a roughly equal volume of acrylic blast media (Type V, 0.42–0.56 mm diameter, Kramer Industries). The bottom-most 6.5 cm of the foam containers were filled with this mixture plus EPS foam pellets 2–4 mm in diameter (LACrafts), which enhanced radiolucency while maintaining relatively consistent bulk material properties. That combination was packed using a rubber mallet to provide a 6.5 cm deep stable base. Three to four 3 mm diameter lead shot were placed slightly below the surface of this stable base, to spatially register substrate volumes during subsequent 3D animation and analyses. Upon this base, the remaining 5 cm of the deformable substrate varied across the three containers. In the first, called the 'firm' condition, the remaining 5 cm was filled with substrate and also packed using a rubber mallet. The remainder of the trackway was covered with rigid, closed-cell EPS panels, as in the carbon fibre condition. In the second variant, an additional 2.5 cm of the 'firm' mud variant was added atop the firm base. Additional water was added to the substrate and this hydrated version was used to fill the uppermost 2.5 cm of the foam container. This variant was called 'hydrated 2.5 mud'[16] or 'wet 2.5 mud' (Fig. 1h). When this substrate was in place, the remainder of the trackway was made flush and level by covering it with 2.5 cm thick panels of soft, deformable upholstery foam. In the third deformable substrate condition, the most superficial 5 cm of the foam container was filled entirely with the hydrated substrate described immediately above. This was termed 'hydrated 5 mud'[16] or 'wet 5 mud' (Fig. 1h). When this was used, the rest of the trackway was made flush and level by covering with 5 cm thick panels of soft, deformable upholstery foam. For each of the three deformable substrate variants, a set of three or four 3 mm diameter lead pellets were also placed on the substrate's surface, visible to both the biplanar X-ray cameras and the 3D scanner (see below) such that a 3D model of the track produced in the substrate could be accurately registered to the scene during 3D animation.

Biplanar X-ray experimental protocol

Four adult subjects were recruited to participate in these experiments and all provided their informed consent following protocols approved by the Institutional Review Boards of Brown University and Chatham University. A marker was used to draw an array of 85 dots across each subject's right foot. Marker dots were placed at anatomical locations of interest (for example, metatarsal heads and navicular tuberosity) but also at intermediate positions to provide roughly uniform coverage across the plantar surface and onto the sides of the foot, as well as on the tops of toes. A handheld structured light scanner (Creaform Go!SCAN 50) was used to collect a 3D scan of each subject's marked foot. Following 3D scanning, 85 radiopaque beads (SureMark) were placed at each of the marker dots and secured using medical adhesive (SkinTac). Beads are sufficiently small that subjects reported limited

ability to sense their presence, particularly while walking on deformable substrates and they reported no discernible influences on their normal foot function. Once beads were secured, subjects walked along the experimental trackway several times until they felt comfortable moving across it.

Each subject completed a minimum of 13 trials. In the first, they stood still with their feet slightly staggered (right in front of left) and their right foot within the biplanar X-ray view. A single pair of X-ray images was captured of their marked foot. Subjects then completed at least three trials walking across each of four substrate variants at a self-selected, comfortable walking speed. If their foot missed the biplanar X-ray camera, they were asked to repeat the trial. After walking through a deformable substrate, the track that a subject left behind was immediately 3D scanned. Most scans were captured with the handheld structured light scanner and processed using Creaform VXElements software (Creaform). However, for some trials (nine), the software was still processing the previous track model and photogrammetry was used instead so as to not delay the experiment. Photographs were taken using a Canon 5D Mark III 22.3-Megapixel camera outfitted with a 50 mm prime lens (Canon) and processed using Agisoft Metashape Professional (v.1.6.4, Agisoft LLC). Both techniques produced 3D models of tracks with submillimetre resolution. After a track had been scanned, the surface beads were removed, the substrate was leveled using a trowel and then the surface beads were again placed on the surface of the substrate.

An additional four adult subjects completed trials with a slightly different protocol in a subsequent year. This protocol was also approved by the Institutional Review Boards of Brown University and Chatham University. Subjects in this later set of experiments also produced tracks while walking at self-selected comfortable speeds through the same substrates and so measurements of RAV from their tracks are included to increase the sample of human observations in Fig. 4.

Three-dimensional animation of biplanar X-ray experiments

Experimental data were animated following the procedures of ref. [16], which were themselves adapted from protocols for X-ray Reconstruction of Moving Morphology (XROMM)[37]. XMALab software (v.1.5.5)[38] was used to undistort and calibrate biplanar X-ray videos and then to compute the 3D trajectories of the radiopaque beads on each subject's foot and on and within the substrate. These 3D motion data were unfiltered, as they were not placed on rigid bodies (both feet and substrates deformed dynamically) and filtering algorithms were therefore more likely to introduce rather than reduce noise or error. Instead, the polynomial fitting procedure of XMALab was used to improve subpixel tracking accuracy and this should have the desired effect of minimizing potential noise/error in 3D bead positions (B. Knörlein, personal communication).

The 3D scans of subjects' feet were exported in .obj format from VXElements software and subsequently imported into Autodesk Maya 2020. The foot models were retopologized from about 73,000–97,000 triangles to 5,000 quads, to improve computation speeds without sacrificing geometric detail. The radiopaque foot beads and their 3D trajectories, were imported as virtual spheres using XROMM MayaTools (v.2.2.3; https://bitbucket.org/xromm/xromm_mayatools/src/master/). The positions of beads on the 3D foot model were directly linked to the positions of imported spheres and interconnected to construct a low-resolution proxy of the foot. The foot model was then linked to the low-resolution proxy using Maya's wrap deformer tool and this allowed the high-resolution 3D foot model to accurately move and deform in concert with the tracked 3D trajectories of the radiopaque beads. For trials on deformable substrates, the radiopaque substrate beads were also imported as virtual spheres using XROMM MayaTools. The 3D scans of tracks were imported in .obj format and manually registered to the scene by matching the positions of surface beads on the track model to their tracked 3D positions.

Within Autodesk Maya, foot trajectories could be directly compared with track positions and used to formulate hypotheses for track arch creation. Within Maya, 3D models of the foot's volumetric sweep through the substrate were generated by using the 'Create animation snapshot' tool and combining the frame-by-frame foot poses into a composite mesh (Supplementary Note 2 and Extended Data Fig. 2).

Marker displacement vectors (Fig. 3c) were visualized in Maya using custom Bifrost Graph compounds. Within an animated sequence, the skin marker positions (acquired from the vertices of the low-resolution foot mesh) from the current frame were subtracted from those of the subsequent frame to calculate 3D displacement vectors. Vectors were rendered as strands; strand magnitudes were scaled up ×20 to improve visibility and were coloured on the basis of their vertical component (red up, blue down). The foot's sagittal pivot was identified in Maya by averaging the coordinates of the subset of sole markers (57; toes excluded) that moved vertically <0.2 mm between the current and subsequent frame. Thresholds of 0.1, 0.3, 0.4 and 0.5 mm showed nearly identical pivot placements and all shared the forward translation pattern.

Particle simulation and track ontogeny

To explore the mechanistic origins of track morphology via track ontogeny[14–16], particle simulations were conducted using the discrete element method (DEM) through LIGGGHTS[39] (Supplementary Videos 1 and 2). A virtual tray measuring 21 × 35 × 8 cm^3 was created in Maya and registered to the same position as the volume of substrate that the foot traversed during the biplanar X-ray experiment. The virtual tray was filled with ~800,000 virtual particles, each measuring 2 mm in diameter. Particle properties (Young's modulus, Poisson ratio, cohesion and friction) were adjusted until macroscopic bulk behaviour of the substrate was similar to the substrate used in biplanar X-ray experiments.

Animations of 3D foot motions were exported from Autodesk Maya and brought into the virtual simulation environment of LIGGGHTS. The simulated feet deform to reproduce the deforming external geometry of the foot, as reconstructed from the biplanar X-ray experimental data (see also ref. [16]). Mesh and vertex positions were interpolated to increase temporal resolution of the foot's motion to 1,000 fps, to mitigate artificially rapid foot and substrate translations and deformations that would occur if simulations were processed at the same 50 fps speed that was used in experimental recording. Simulation data were visualized using OVITO (v.3.0.0)[40].

Quantifying foot and track arch volumes

A new tool for quantitative, 3D volumetric measurement of arch height from both feet and tracks was also developed in Maya. Foot and/or track 3D models were imported and virtual points were placed at the approximate positions of the first and fifth metatarsophalangeal joints and centrally beneath the heel (Fig. 1e). These points defined the inferior corners of a right triangular prism, whose height was adjusted such that it extended above the track surface or the foot's plantar surface. A Boolean intersection was used to extract a 3D model of the volume that was enclosed by the prism and the track (Fig. 1f) or foot (Fig. 1g).

RAV was calculated as 100 times the cube root of either Boolean arch model's volume divided by the square root of the prism base's area.

$$\mathrm{RAV} = 100 \times \left(\sqrt[3]{\text{arch volume}} \div \sqrt{\text{prism base area}} \right)$$

Standardization by area permits the comparison of longitudinal arch volumes across tracks that differ in absolute size. This is necessary for comparing similarly shaped tracks that differ in length, such as those from Laetoli and those from modern humans. The longitudinal arches of tracks that differ in width can also be compared, including those that differ in their degrees of hallucial abduction (for example, the chimpanzee tracks compared with hominin tracks in Fig. 4a).

To evaluate this measurement tool, we also assessed inter-observer variation. Two observers (K.G.H. and P.L.F.) independently placed landmarks and measured RAVs from 37 track and 4 foot models. Paired *t*-tests (using R v.4.1.0)[41] showed that across this sample, measurements of RAV were not significantly different between the two observers ($t = -1.48$, $P = 0.15$; Extended Data Fig. 5). The average inter-observer difference was 0.42, with a 95% confidence interval of −1.00 to 0.15. In other words, the average difference between observers is ~1% or less of the RAVs that we measured for human experimental tracks (Fig. 4a).

Additional track arch variables

The track arch axis was a line segment spanning from the heel landmark to the midpoint between metatarsophalangeal landmarks (Fig. 1e). We aligned each track 3D model such that the surrounding, undisturbed substrate corresponded to the X–Y plane in 3D space. Absolute depth of each track was measured at the midpoint of its arch axis and we defined 'relative depth' as the absolute depth of the midpoint of the track arch axis divided by the length of its arch axis.

'Pitch' was defined as the minimum 3D angle of the track arch axis with respect to horizontal. A track with a positive pitch has the heel landmark deeper than the metatarsophalangeal midpoint (nose up). A track with negative pitch has the metatarsophalangeal midpoint deeper than the heel landmark (nose down). A horizontal track arch axis has a pitch of 0°.

Modern and fossil track analyses

Samples of Laetoli, Ileret and Walvis Bay fossil tracks and habitually barefoot human and chimpanzee experimental tracks, were all measured using the same arch quantification tool that was developed here in Autodesk Maya. Track models were imported to Maya in .obj format and subsequently measured using the procedures described above. Tracks were excluded from fossil samples if erosional damage, overprinting or taphonomic effects were evident in the 3D model and prevented arch measurement.

Our experimental results (Fig. 1h) and those of others[22] have demonstrated that track arch morphology is influenced by track depth. Fossil tracks and other experimental tracks were included in comparative plots as long as their absolute depths (defined above) were within two standard deviations of the mean absolute depth observed in deep mud tracks from our human biplanar X-ray experiments ('wet 2.5' and 'wet 5' conditions).

First-generation casts of the Laetoli G1 tracks ($n = 11$) housed at the National Museums of Kenya were previously digitized by K.G.H. using photogrammetry[10]. Laetoli S1 ($n = 2$) and A tracks ($n = 1$) were freely available via MorphoSource (www.morphosource.org)[20,23]. Ileret tracks ($n = 11$ from five trackways; reduced to $n = 4$ from three trackways after filtering by depth) were also digitized by K.G.H. using photogrammetry, with photographs taken immediately following their excavation[21]. Models of Walvis Bay tracks were made freely available online by M. Bennett through NERC grant NE/HOO4211/1 (http://footprints.bournemouth.ac.uk/) and are described in detail by ref. [22]. From this site we focused on the tracks from 'Trail One' and 'Trail Two', as these sampled a broad range of substrate conditions encompassing the range of track depths observed in our biplanar X-ray experiments ($n_1 = 19$ and $n_2 = 13$; reduced to $n_1 = 13$ and $n_2 = 11$ after filtering by depth). Tracks produced by habitually unshod humans were collected by K.G.H. in a previous study[17]. Briefly, these experiments involved people making tracks while walking at a variety of speeds through hydrated mud, made from the same sediments in which fossil tracks at Ileret are preserved. A subset of those tracks, produced by people walking at comfortable, self-selected walking speeds, were included here for comparison ($n = 69$ tracks from 24 subjects; reduced to $n = 36$ tracks from 17 subjects after filtering by depth). Bipedal chimpanzee tracks were also collected by K.G.H. in a previous study[10] ($n_1 = 24$ and $n_2 = 21$; $n_1 = 22$, $n_2 = 21$ after filtering by depth).

Plots to compare experimental and fossil tracks were generated using R v.4.1.0 (ref. [41]), including the dplyr and ggplot2 packages[42,43].

Reporting summary

Further information on research design is available in the Nature Portfolio Reporting Summary linked to this article.

Data availability

Raw data from biplanar X-ray experiments are publicly available through the XMAPortal at the following link: https://xmaportal.org/webportal/larequest.php?request=CollectionView&StudyID=43&instit=BROWN&collectionID=20.

Code availability

Source data and code used to generate the figures in this manuscript are publicly available at the following address: https://doi.org/10.6084/m9.figshare.20736697.

References

1. Darwin, C. *The Descent of Man, and Selection in Relation to Sex* (J. Murray, 1871).
2. Morton, D. J. Evolution of the longitudinal arch of the human foot. *J. Bone Jt Surg.* **6**, 56–90 (1924).
3. Holowka, N. B. & Lieberman, D. E. Rethinking the evolution of the human foot: insights from experimental research. *J. Exp. Biol.* **221**, jeb174425 (2018).
4. Bramble, D. M. & Lieberman, D. E. Endurance running and the evolution of *Homo*. *Nature* **432**, 345–352 (2004).
5. Leakey, M. D. & Hay, R. L. Pliocene footprints in the Laetolil Beds at Laetoli, northern Tanzania. *Nature* **278**, 317–323 (1979).
6. Day, M. H. & Wickens, E. H. Laetoli Pliocene hominid footprints and bipedalism. *Nature* **286**, 385–387 (1980).
7. White, T. D. & Suwa, G. Hominid footprints at Laetoli: facts and interpretations. *Am. J. Phys. Anthropol.* **72**, 485–514 (1987).
8. Raichlen, D. A., Gordon, A. D., Harcourt-Smith, W. E. H., Foster, A. D. & Haas, W. R. Laetoli footprints preserve earliest direct evidence of human-like bipedal biomechanics. *PLoS ONE* **5**, e9769 (2010).
9. Crompton, R. H. et al. Human-like external function of the foot, and fully upright gait, confirmed in the 3.66 million year old Laetoli hominin footprints by topographic statistics, experimental footprint-formation and computer simulation. *J. R. Soc. Interface* **9**, 707–719 (2012).
10. Hatala, K. G., Demes, B. & Richmond, B. G. Laetoli footprints reveal bipedal gait biomechanics different from those of modern humans and chimpanzees. *Proc. R. Soc. B* **283**, 20160235 (2016).
11. Bennett, M. R. et al. Early hominin foot morphology based on 1.5-million-year-old footprints from Ileret, Kenya. *Science* **323**, 1197–1201 (2009).
12. Ward, C. V., Kimbel, W. H. & Johanson, D. C. Complete fourth metatarsal and arches in the foot of *Australopithecus afarensis*. *Science* **331**, 750–753 (2011).
13. Pontzer, H. et al. Locomotor anatomy and biomechanics of the Dmanisi hominins. *J. Hum. Evol.* **58**, 492–504 (2010).
14. Falkingham, P. L. & Gatesy, S. M. The birth of a dinosaur footprint: subsurface 3D motion reconstruction and discrete element simulation reveal track ontogeny. *Proc. Natl Acad. Sci. USA* **111**, 18279–18284 (2014).
15. Falkingham, P. L., Turner, M. L. & Gatesy, S. M. Constructing and testing hypotheses of dinosaur foot motions from fossil tracks using digitization and simulation. *Palaeontology* **63**, 865–880 (2020).

16. Hatala, K. G., Gatesy, S. M. & Falkingham, P. L. Integration of biplanar X-ray, three-dimensional animation and particle simulation reveals details of human 'track ontogeny'. *Interface Focus* **11**, 20200075 (2021).
17. Hatala, K. G. et al. Footprints reveal direct evidence of group behavior and locomotion in *Homo erectus*. *Sci. Rep.* **6**, 28766 (2016).
18. Usherwood, J. R., Channon, A. J., Myatt, J. P., Rankin, J. W. & Hubel, T. Y. The human foot and heel–sole–toe walking strategy: a mechanism enabling an inverted pendular gait with low isometric muscle force? *J. R. Soc. Interface* **9**, 2396–2402 (2012).
19. Webber, J. T. & Raichlen, D. A. The role of plantigrady and heel-strike in the mechanics and energetics of human walking with implications for the evolution of the human foot. *J. Exp. Biol.* **219**, 3729–3737 (2016).
20. Masao, F. T. et al. New footprints from Laetoli (Tanzania) provide evidence for marked body size variation in early hominins. *eLife* **5**, e19568 (2016).
21. Hatala, K. G. et al. Hominin track assemblages from Okote Member deposits near Ileret, Kenya, and their implications for understanding fossil hominin paleobiology at 1.5 Ma. *J. Hum. Evol.* **112**, 93–104 (2017).
22. Morse, S. A. et al. Holocene footprints in Namibia: the influence of substrate on footprint variability. *Am. J. Phys. Anthropol.* **151**, 265–279 (2013).
23. McNutt, E. J. et al. Footprint evidence of early hominin locomotor diversity at Laetoli, Tanzania. *Nature* **600**, 468–471 (2021).
24. Zeininger, A., Schmitt, D. & Wunderlich, R. E. Mechanics of heel-strike plantigrady in African apes. *J. Hum. Evol.* **145**, 102840 (2020).
25. Elftman, H. & Manter, J. Chimpanzee and human feet in bipedal walking. *Am. J. Phys. Anthropol.* **20**, 69–79 (1935).
26. Latimer, B. & Lovejoy, C. O. The calcaneus of *Australopithecus afarensis* and its implications for the evolution of bipedality. *Am. J. Phys. Anthropol.* **78**, 369–386 (1989).
27. Prang, T. C. Calcaneal robusticity in Plio-Pleistocene hominins: implications for locomotor diversity and phylogeny. *J. Hum. Evol.* **80**, 135–146 (2015).
28. Fernández, P. J. et al. Evolution and function of the hominin forefoot. *Proc. Natl Acad. Sci. USA* **115**, 8746–8751 (2018).
29. Venkadesan, M. et al. Stiffness of the human foot and evolution of the transverse arch. *Nature* **579**, 97–100 (2020).
30. Latimer, B. & Lovejoy, C. O. Hallucal tarsometatarsal joint in *Australopithecus afarensis*. *Am. J. Phys. Anthropol.* **82**, 125–133 (1990).
31. DeSilva, J. M., Gill, C. M., Prang, T. C., Bredella, M. A. & Alemseged, Z. A nearly complete foot from Dikika, Ethiopia and its implications for the ontogeny and function of *Australopithecus afarensis*. *Sci. Adv.* **4**, eaar7723 (2018).
32. DeSilva, J. M. et al. Midtarsal break variation in modern humans: functional causes, skeletal correlates, and paleontological implications. *Am. J. Phys. Anthropol.* **156**, 543–552 (2015).
33. Kelly, L. A., Cresswell, A. G., Racinais, S., Whiteley, R. & Lichtwark, G. Intrinsic foot muscles have the capacity to control deformation of the longitudinal arch. *J. R. Soc. Interface* **11**, 20131188 (2014).
34. Kelly, L. A., Lichtwark, G. & Cresswell, A. G. Active regulation of longitudinal arch compression and recoil during walking and running. *J. R. Soc. Interface* **12**, 20141076 (2015).
35. Holowka, N. B., Richards, A., Sibson, B. E. & Lieberman, D. E. The human foot functions like a spring of adjustable stiffness during running. *J. Exp. Biol.* **224**, jeb219667 (2021).
36. Wood, B. & Collard, M. The human genus. *Science* **284**, 65–71 (1999).
37. Brainerd, E. L. et al. X-ray reconstruction of moving morphology (XROMM): precision, accuracy and applications in comparative biomechanics research. *J. Exp. Zool.* **313A**, 262–279 (2010).
38. Knörlein, B. J., Baier, D. B., Gatesy, S. M., Laurence-Chasen, J. D. & Brainerd, E. L. Validation of XMALab software for marker-based XROMM. *J. Exp. Biol.* **219**, 3701–3711 (2016).
39. Kloss, C. & Goniva, C. in *Supplemental Proceedings: Materials Fabrication, Properties, Characterization, and Modeling* Vol. 2 (ed. TMS) 781–788 (John Wiley & Sons, 2011).
40. Stukowski, A. Visualization and analysis of atomistic simulation data with OVITO—the Open Visualization Tool. *Model. Simul. Mater. Sci. Eng.* **18**, 015012 (2010).
41. R Core Team. *R: A Language and Environment for Statistical Computing* (R Foundation for Statistical Computing, 2019).
42. Wickham, H., François, R., Henry, L. & Müller, K. dplyr: A grammar of data manipulation. R package version 1.0.7 (2019).
43. Wickham, H. *ggplot2: Elegant Graphics for Data Analysis* (Springer-Verlag, 2016).

Acknowledgements

We thank D. Baier, B. Brainerd, S. Cheleden, F. Drury, K. Fiske, K. Huffman, B. Knörlein, D. Laidlaw, K. Tani Little, S. Megherhi, J. Novotny, D. North, M. Turner and the students of CS137 for assistance directly related to the design and implementation of this project. We thank the anonymous volunteers who participated in biplanar X-ray experiments. We are grateful to A. Manafzadeh for feedback at many stages of analysis. Discrete element simulations were made possible through a PRACE allocation of supercomputer resources (project 2021250007, Irene-Rome). This study received funding support from the National Science Foundation (BCS-1825403 to K.G.H. and P.L.F.; BCS-1824821 to S.M.G.) and from the Chatham University Research & Sabbatical Committee (to K.G.H.).

Author contributions

All authors participated in the conceptualization, planning and administration of this project. K.G.H. and S.M.G. carried out biplanar X-ray experiments with input from P.L.F. P.L.F. carried out discrete element simulations with input from K.G.H. and S.M.G. All authors participated in analysing the data and in writing and editing the manuscript.

Competing interests

The authors declare no competing interests.

Additional information

Extended data is available for this paper at https://doi.org/10.1038/s41559-022-01929-2.

Supplementary information The online version contains supplementary material available at https://doi.org/10.1038/s41559-022-01929-2.

Correspondence and requests for materials should be addressed to Kevin G. Hatala.

Peer review information *Nature Ecology & Evolution* thanks the anonymous reviewers for their contribution to the peer review of this work.

https://doi.org/10.1038/s41559-022-01929-2

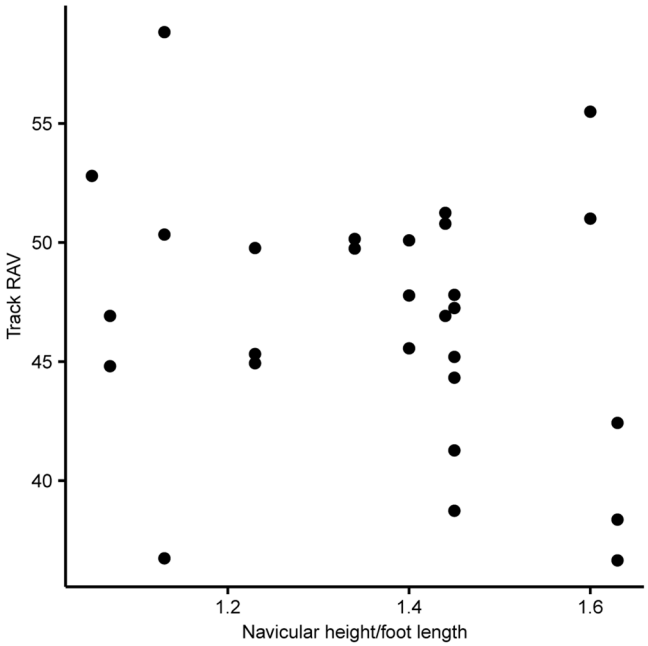

Extended Data Fig. 1 | Track RAV and navicular height. Within this previously published experimental data set[17] (Supplementary Note 1), we observed no statistically significant relationship between track RAV and relative navicular height (navicular height/foot length).

https://doi.org/10.1038/s41559-022-01929-2

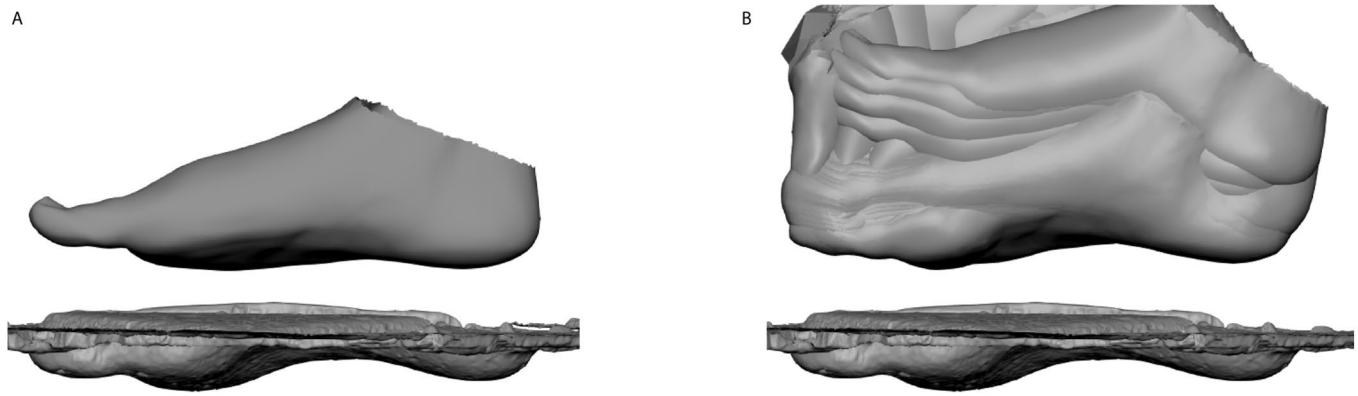

Extended Data Fig. 2 | Origins of kinematic hypotheses. (**a**) Maya visualization of the foot at midstance directly above the track that this foot produced during a walking trial. (**b**) An 'animation snapshot' positioned at the same height as the foot in A, directly above the 3-D model of the track that this foot and its motion produced. The foot at midstance is relatively flat compared with the longitudinally arched track. However, the animation snapshot and the track are similarly arched. A sequence of similar observations led us to hypothesize that track arch morphology was a product of foot kinematics and not foot anatomy.

https://doi.org/10.1038/s41559-022-01929-2

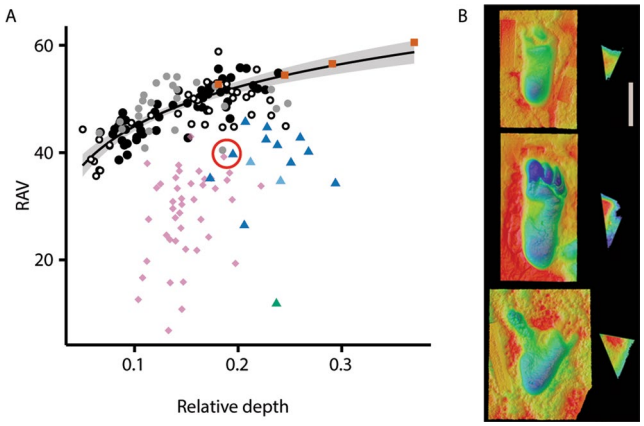

Extended Data Fig. 3 | RAVs and morphologies of human and chimpanzee tracks. (**a**) As an example we focus on one Laetoli track, one Walvis Bay track and one experimental chimpanzee track, with similar RAV and relative depth measurements (red circle). (**b**) The morphologies of the two hominin tracks and their respective arch models are similar to each other and readily distinguished from those of the bipedal chimpanzee (all models from right feet). The arch volume of hominin tracks is concentrated beneath the medial midfoot, while that of the bipedal chimpanzee track is concentrated distally, in between the first and second rays. Thus, the hominin tracks are arched longitudinally, while the bipedal chimpanzee track is not. Two different colour scales are applied to map relative heights, one for tracks and one for arch models, to optimize visualization of each set. Scale bar at right is 10 cm.

https://doi.org/10.1038/s41559-022-01929-2

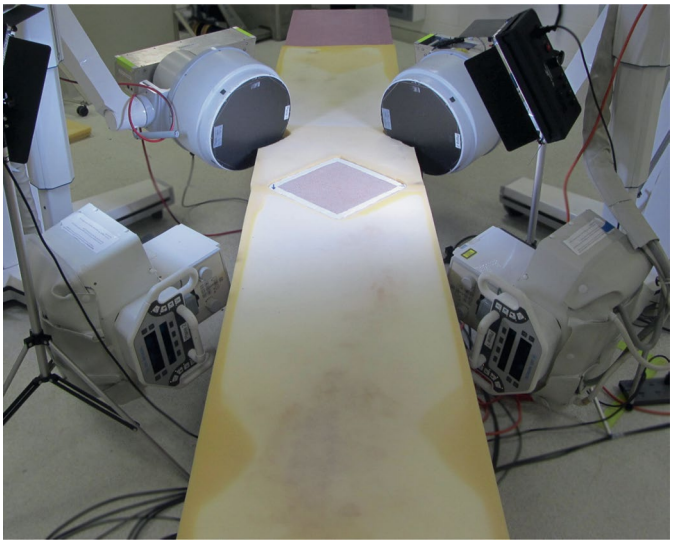

Extended Data Fig. 4 | Photograph of trackway setup used for biplanar X-ray experiments. Two X-ray emitters (foreground) project overlapping collimated X-rays that are received by two circular image intensifiers (background) equipped with video cameras. At the intersection of the biplanar X-ray beams is a container that is filled with mud ('wet 5' variety pictured here). Atop the remainder of the trackway is a deformable foam whose thickness matches the depth of mud within the container, which therefore allows subjects to sink to a similar extent with each step.

https://doi.org/10.1038/s41559-022-01929-2

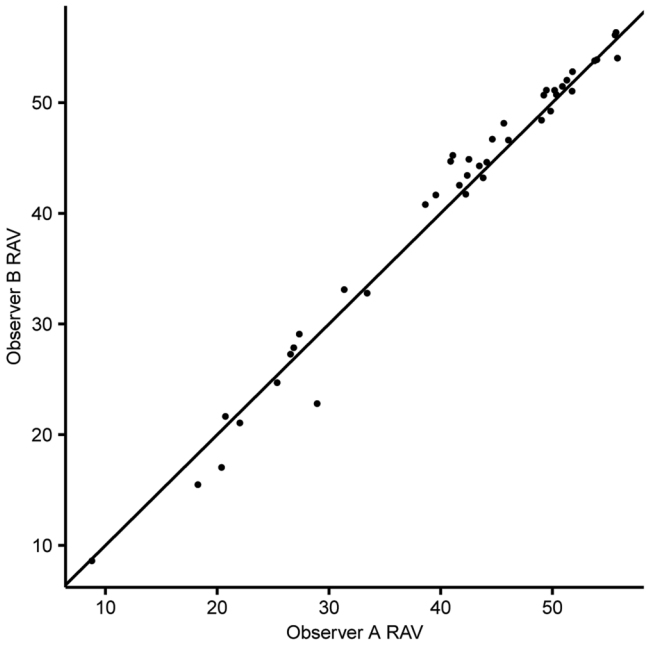

Extended Data Fig. 5 | Interobserver variation in RAV measurements from track and foot 3-D models. Paired observations and line of identity are plotted. Average interobserver difference was 0.42 (95% confidence interval of −1.00 to 0.15). RAV measurements were more consistent between observers for deeper tracks.

nature portfolio

Corresponding author(s): Kevin G. Hatala

Last updated by author(s): Sep 28, 2022

Reporting Summary

Nature Portfolio wishes to improve the reproducibility of the work that we publish. This form provides structure for consistency and transparency in reporting. For further information on Nature Portfolio policies, see our Editorial Policies and the Editorial Policy Checklist.

Statistics

For all statistical analyses, confirm that the following items are present in the figure legend, table legend, main text, or Methods section.

n/a	Confirmed
☐	☒ The exact sample size (*n*) for each experimental group/condition, given as a discrete number and unit of measurement
☐	☒ A statement on whether measurements were taken from distinct samples or whether the same sample was measured repeatedly
☐	☒ The statistical test(s) used AND whether they are one- or two-sided *Only common tests should be described solely by name; describe more complex techniques in the Methods section.*
☒	☐ A description of all covariates tested
☒	☐ A description of any assumptions or corrections, such as tests of normality and adjustment for multiple comparisons
☐	☒ A full description of the statistical parameters including central tendency (e.g. means) or other basic estimates (e.g. regression coefficient) AND variation (e.g. standard deviation) or associated estimates of uncertainty (e.g. confidence intervals)
☐	☒ For null hypothesis testing, the test statistic (e.g. *F*, *t*, *r*) with confidence intervals, effect sizes, degrees of freedom and *P* value noted *Give P values as exact values whenever suitable.*
☒	☐ For Bayesian analysis, information on the choice of priors and Markov chain Monte Carlo settings
☒	☐ For hierarchical and complex designs, identification of the appropriate level for tests and full reporting of outcomes
☐	☒ Estimates of effect sizes (e.g. Cohen's *d*, Pearson's *r*), indicating how they were calculated

Our web collection on statistics for biologists contains articles on many of the points above.

Software and code

Policy information about availability of computer code

Data collection	Biplanar X-ray videos were analyzed using XMALab (v.1.5.5). Tracked marker 3D coordinates were imported to Autodesk Maya (v.2020) and animations were derived using XROMM Maya Tools (v.2.2.3). Animated trials were used to drive DEM simulations in LIGGGHTS (v.3.8.0), which were subsequently visualized using OVITO (v.3.0.0).
Data analysis	Autodesk Maya (v.2020) and OVITO (v.3.0.0) were used to analyze track formation dynamics. R (v.4.1.0) was used to generate plots, and scripts included functions from the dplyr (v.1.0.7) and ggplot2 (v.3.3.5) packages.

For manuscripts utilizing custom algorithms or software that are central to the research but not yet described in published literature, software must be made available to editors and reviewers. We strongly encourage code deposition in a community repository (e.g. GitHub). See the Nature Portfolio guidelines for submitting code & software for further information.

Data

Policy information about availability of data

All manuscripts must include a data availability statement. This statement should provide the following information, where applicable:

- Accession codes, unique identifiers, or web links for publicly available datasets
- A description of any restrictions on data availability
- For clinical datasets or third party data, please ensure that the statement adheres to our policy

All processed data that led to the conclusions of this study are available in the main text or the supplementary materials. Source data and code used to generate the figures in this manuscript are publicly available at the following address: https://doi.org/10.6084/m9.figshare.20736697. Raw data are publicly available through the XMAPortal at the following link: https://xmaportal.org/webportal/larequest.php?request=CollectionView&StudyID=43&instit=BROWN&collectionID=20.

Field-specific reporting

Please select the one below that is the best fit for your research. If you are not sure, read the appropriate sections before making your selection.

☐ Life sciences ☐ Behavioural & social sciences ☒ Ecological, evolutionary & environmental sciences

For a reference copy of the document with all sections, see nature.com/documents/nr-reporting-summary-flat.pdf

Ecological, evolutionary & environmental sciences study design

All studies must disclose on these points even when the disclosure is negative.

Study description	The study involved biplanar X-ray experiments aimed at understanding how arched footprints are formed when humans walk on deformable substrates. Mechanistic processes observed in these experiments were deciphered using 3-D animation and discrete element particle simulation. Experimental footprints were then compared with fossil hominin footprints, and with footprints created by chimpanzees, to understand whether those record similar patterns of foot mechanics.
Research sample	The experimental research sample included eight young adults (7 female, 1 male, all in their early to mid-twenties). Each subject's feet were recorded via biplanar X-ray video as they walked a minimum of three times across each of four substrates (rigid carbon fiber, "firm" mud, "wet 2.5" mud, "wet 5" mud). In trials where subjects produced footprints, these were digitized using photogrammetry or a structured light 3-D scanner. Experimental chimpanzee tracks, and the Laetoli G1 tracks, were digitized by K.G.H. using photogrammetry, as part of a previously published study (Hatala et al., 2016). Laetoli S1 and A tracks were accessed through Morphosource (www.morphosource.org). Ileret tracks were also digitized by K.G.H. using photogrammetry, following their excavation as part of an earlier study (Hatala et al., 2017). Models of Walvis Bay tracks were made freely available online by Professor Matthew Bennett through NERC grant NE/HOO4211/1 (http://footprints.bournemouth.ac.uk/) and have been described by Morse et al. (2013). Analyses also included experimental human footprints collected in a previously published study (Hatala et al., 2016); that sample included 69 footprints made by 24 subjects, ranging widely in age from children to adults (ages 4-47).
Sampling strategy	Experimental sample size was determined by the feasibility of data processing and by the clarity of observations of track formation processes. Biplanar imaging and particle simulation are immensely time-consuming, such that large sample sizes are impractical. Here, the clarity of the observed patterns of arch formation did not necessitate additional data collection. Sample sizes of fossil hominin tracks were determined based on data availability and the nature of track preservation - as many tracks as possible were included for each of the samples analyzed.
Data collection	Biplanar X-ray experiments were conducted, and videos were digitized and animated, by K.G.H. and S.M.G. Discrete element particle simulations were conducted by P.L.F. Both K.G.H. and P.L.F. measured experimental tracks in order to assess interobserver error. Fossil hominin tracks were measured by K.G.H.
Timing and spatial scale	Biplanar X-ray experiments were conducted from June 25-28, 2019. A second set of experimental data, which was included in only a single analysis (Fig. 4), was collected from July 26-29, 2021.
Data exclusions	Some fossil hominin tracks were excluded from the analyses shown in Figure 4, and some experimental tracks were excluded from Extended Data Figure 1. Because our experiments (and others) show that track arch morphology is influenced by track depth, we restrict our arch comparisons to tracks of similar depth. Tracks were included in Figure 4 and Extended Data Figure 1 only if their absolute depths were within two standard deviations of the mean depths observed in deep mud tracks from our human experiments.
Reproducibility	All data analyzed here are made publicly available, and the methods used to analyze them are described in detail. We did evaluate interobserver error in measurements of track and foot arches (Extended Data Fig. 5), and found interobserver differences to have minimal impact on results.
Randomization	Randomization was not relevant to our study because we were interested in understanding the mechanistic processes that led to specific patterns of track development, and in inter-group comparisons of footprint samples.
Blinding	Blinding was not relevant to our study, as human subjects had no prior knowledge of our plans to study the mechanics of track arch formation.

Did the study involve field work? ☐ Yes ☒ No

Reporting for specific materials, systems and methods

We require information from authors about some types of materials, experimental systems and methods used in many studies. Here, indicate whether each material, system or method listed is relevant to your study. If you are not sure if a list item applies to your research, read the appropriate section before selecting a response.

Materials & experimental systems

n/a	Involved in the study
☒	☐ Antibodies
☒	☐ Eukaryotic cell lines
☐	☒ Palaeontology and archaeology
☒	☐ Animals and other organisms
☐	☒ Human research participants
☒	☐ Clinical data
☒	☐ Dual use research of concern

Methods

n/a	Involved in the study
☒	☐ ChIP-seq
☒	☐ Flow cytometry
☒	☐ MRI-based neuroimaging

Palaeontology and Archaeology

Specimen provenance	No new fossils were excavated or collected for this study. All material analyzed here has been published previously.
Specimen deposition	The specimens measured here have been published previously and details on availability are provided in those original publications.
Dating methods	No new dates are provided here.

☐ Tick this box to confirm that the raw and calibrated dates are available in the paper or in Supplementary Information.

Ethics oversight	Ethical oversight was not relevant here because the study only required access to previously published data.

Note that full information on the approval of the study protocol must also be provided in the manuscript.

Human research participants

Policy information about studies involving human research participants

Population characteristics	Data were collected from 8 healthy young adults (7 female, 1 male, all in their early twenties), without any foot or lower limb maladies, or injury/surgical histories, that might impact their foot function. Due to the exposure to small amounts of X-ray radiation, subjects were also excluded if there was any chance of pregnancy.
Recruitment	Participants were recruited via e-mail. We did not identify any potential for recruitment bias that could impact results.
Ethics oversight	Ethical approval was provided by the Brown University and Chatham University Institutional Review Boards.

Note that full information on the approval of the study protocol must also be provided in the manuscript.